04.1

Investigation of parameters of high-pressure volumetric discharge at pulse repetition rate up to 100 kHz

© P.A. Bokhan[1], P.P. Gugin[1], D.E. Zakrevsky[1,2], M.A. Lavrukhin[1]

[1] Rzhanov Institute of Semiconductor Physics, Siberian Branch, Russian Academy of Sciences, Novosibirsk, Russia
[2] Novosibirsk State Technical University, Novosibirsk, Russia
E-mail: zakrdm@isp.nsc.ru

Received May 15, 2024
Revised June 4, 2024
Accepted June 4, 2024

The characteristics of a wide-aperture volumetric gas discharge in helium in a 60 cm^3 cuvette at gas pressure up to atmospheric pressure under excitation by pulses with voltage rise fronts less than 5 ns and pulse repetition rate up to 100 kHz have been investigated. At atmospheric pressure the volumetric character of pulse current with amplitude up to 50 A, peak power up to 2 MW and average power up to 1.3 kW was obtained.

Keywords: gas discharge, high pressure, helium, pulse excitation, high pulse repetition rate.

DOI: 10.61011/TPL.2024.10.59684.19992

The present study is focused on advancing the technology of high-energy high-voltage electrophysical devices operating in the nano- and subnanosecond ranges. The aim of the study is to examine a wide-aperture pulsed gas discharge in helium at a pressure up to 1 atm and a pulse repetition rate up to 100 kHz. Such discharges (high-pressure discharges with volumetric current flow in inert and molecular gases) are of interest as a means of energy deposition into the active media of gas lasers and dissociation of complex gaseous chemical compounds, in high-speed high-voltage switches and sources of charged particles, in pulsed sources of high-frequency oscillations, in plasma-chemical and plasma-biological reactors, etc. (see, e.g., [1–3]). The capacity for operation with volumetric discharge current flow at a high pulse repetition rate (tens or hundreds of kilohertz) is essential in this context. This may be achieved by initiating a discharge with high-voltage pulses shorter than the time of propagation of the ionization wave through the discharge gap. This imposes requirements on the rise time ($\sim$ kV/(cm·ns)) and the duration (several nanoseconds or tens of nanoseconds) of a voltage pulse.

A cuvette (Fig. 1, *a*) with planar polished electrodes *1*, *1'* with an open part diameter of 5.6 cm and an interelectrode distance of 2.4 cm (the discharge volume was 60 cm^3) was used in discharge experiments. The thickness of limited-conductivity electrodes made of reaction-sintered silicon carbide (SiC) was 8 mm, and the resistivity was 0.5$-$1 Ω·cm. Copper contacts *2* were positioned on the outer electrode surface. Dielectric plate *3* made of Al_2O_3 ceramics with a thickness of 2 mm was glued to one of these contacts. Auxiliary plate electrode *4* made of titanium was secured to the other side of ceramic plate *3*. Capacitance $C_d \approx 70$ pF was formed between plates *2* and *4* as a result. The intrinsic capacitance of the discharge cuvette was ~ 6 pF. Voltage needed to excite a discharge could be supplied in two modes: between electrodes *4*$-$*1'* (mode *A* with the inclusion of capacitance C_d; it was assumed that C_d would curb sparking and improve the discharge stability, establishing such conditions under which volumetric current flow is maintained) and directly between electrodes *1*$-$*1'* (mode *B* with capacitance C_d excluded).

The used pulsed power supply featured a transistor generator with a step-up transformer, a magnetic compression line, and a switch. Its design is similar to the one discussed in [4]. To ensure rapid voltage rise across the discharge gap, an eptron, is a discharge device relying in its operation on the buildup of current in the course of breakdown of a capillary discharge structure with a plasma cathode [5], was used as a switch. The design of the eptron is presented in Fig. 1, *b*. It features a cylindrical SiC cathode with an internal diameter of 28 mm and a length of 25 mm. A capillary slit discharge structure 50 mm in length was mounted on one side of the cathode. This structure was a dielectric channel of the Square wave type with a pitch of 3 mm and a slit cross section of 0.3 × 15 mm. The geometry of the slit limited the potential for generation of runaway electrons with an energy sufficient for propagation along the entire length of the capillary from the plasma cathode to the anode and maintained the conditions suitable for rapid plasma recombination in the interpulse period. A grounded metal screen (not shown in Fig. 1, *b*) was mounted outside the capillary structure. The anode was positioned at one end of the capillary structure. On the other side of the eptron cathode, an additional electrode, which allowed one to apply an ignition pulse, was installed to facilitate the buildup of current.

Experiments were carried out with the application of pulse bursts with a period of 0.1 s and rate $f = 5-100$ kHz of filling with regular pulses. These bursts were ~ 20 pulses in length. The examination of dynamics of variation of pulses revealed that their parameters stabilized at the second (third) pulse and remained constant through to the end of a

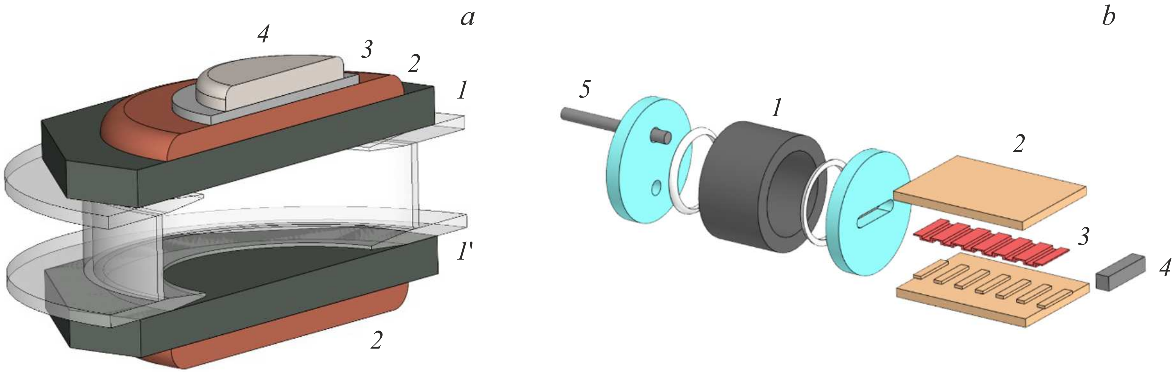

Figure 1. *a* — Discharge cuvette design: *1*, *1′* — SiC electrodes, *2* — copper contacts, *3* — Al_2O_3 plate, and *4* — auxiliary electrode. *b* — Eptron design: *1* — SiC cathode, *2* — capillary discharge structure, *3* — current flow region, *4* — anode, and *5* — additional electrode.

burst. All measurements were performed for the last pulse in a burst.

Helium and hydrogen were used as working media for the eptron. It was found that shorter switching times (~ 1 ns) are achieved in helium. However, hydrogen filling turned out to be more convenient, since discharge development delay τ_d (the time from the moment when 0.1 of the peak cell voltage was reached to the onset of current rise) changed only slightly within a wide range of pulse repetition rates. This enabled operation under a variety of conditions without the need to rearrange magnetic compression links in the primary power supply circuits. Figure 2 shows the functional parameters of the eptron at hydrogen pressure $p_{H_2} = 1.1$ Torr in operation with an active load: the dependences of discharge development delay $\tau_d(f)$, current amplitude $I_e(f)$, and current pulse rise time $\tau_s(f)$ (at the 0.1–0.9 level) on repetition rate f at voltage pulse amplitude $U = 17.5$ kV. An ignition pulse with an energy up to 0.1 J (discharge of the $C = 2$ nF capacitance at a charging voltage up to 10 kV) had little effect on the eptron characteristics at repetition rates up to $f \approx 70$ kHz, but contributed to more stable operation of the device at higher rates. It can be seen from Fig. 2 that eptron discharge delay time τ_d decreases from 180 to 130 ns as f increases from 20 to 100 kHz; the amplitude and the rise time of a current pulse change only slightly in these conditions ($I_e \sim 140$–120 A and $\tau_s = 3.5$–2.7 ns, respectively). Delay times of $\tau_d \approx 100$ ns and shorter (with a tendency to significant τ_d reduction with increasing voltage and pulse repetition rate) are typical for hydrogen pressures $p_{H_2} \approx 2$–4 Torr at $f \sim 5$–60 kHz; therefore, increased pressures $p_{H_2} > 1.1$ Torr were not used, although they led to reduced $\tau_s \leq 2$ ns.

A discharge was initiated in the cuvette (Fig. 1, *a*) by discharging working capacitance $C_0 = 75$ pF through the eptron. Pulses of voltage U (at electrodes *1*–*1′*) and discharge current I (through the shunt in the electrode *2*–ground circuit) were recorded. The amplitude of voltage pulses across the discharge gap varied within the

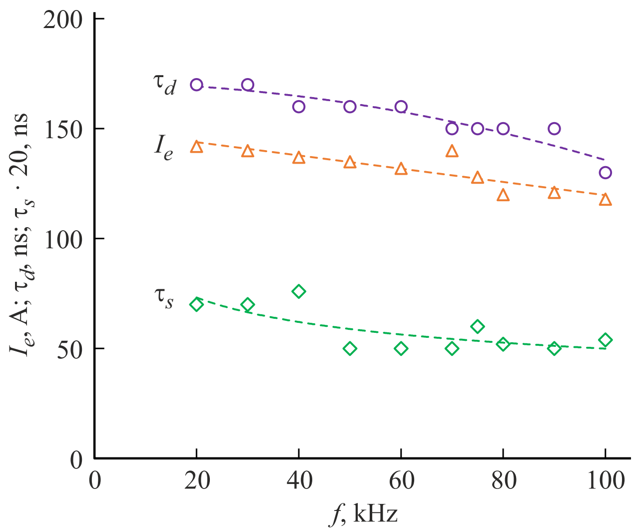

Figure 2. Key eptron parameters as functions of the pulse repetition rate: $\tau_d(f)$, $I_e(f)$, and $\tau_s(f)$. $U = 17.5$ kV, $p_{H_2} = 1.1$ Torr.

$U = 2$–24 kV range, the working gas (helium) pressure was up to $p_{He} \approx 1$ atm.

When voltage is applied to the electrodes, current starts flowing in the discharge gap, and the nature of the discharge depends on the power connection mode. Typical oscillograms of voltage U and discharge current I are presented in Figs. 3, *a* and *b*; as an example, see the curves for $p_{He} \approx 50$ Torr and $f = 65$ kHz (Fig. 3, *a*, modes *A*, *B*) and $p_{He} \approx 450$ Torr and $f = 95$ kHz (Fig. 3, *b*, mode *A*). The first peak in the oscillograms of current is the charging current of the intrinsic capacitance of the discharge cuvette. The characteristic voltage pulse rise times (at the 0.1–0.9 level) are $\tau_U \approx 3$–4 ns (the rate of voltage rise is up to 5 kV/ns). It can be seen that the voltage at electrode *1* remains virtually constant after the passage of a current pulse when U is applied to electrodes *4*–*1′* with capacitance C_d included (mode *A*), since C_d is discharged exclusively through the resistance of

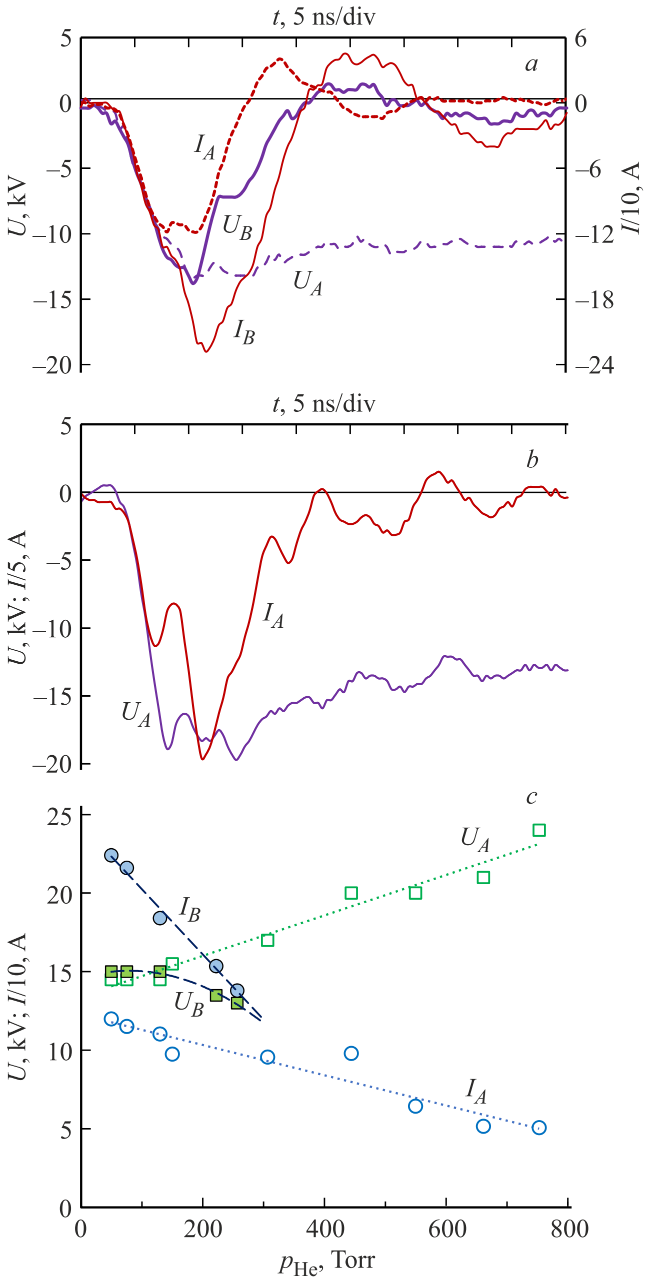

Figure 3. *a* — Oscillograms of voltage U and current I in modes A and B at $p_{He} = 50$ Torr, $f = 65$ kHz; *b* — oscillograms of voltage U and current I in mode A at $p_{He} = 450$ Torr, $f = 95$ kHz; *c* — dependences of peak values of voltage U and current I in modes A and B at $f = 95$ kHz on helium pressure p_{He}.

the voltage sensor and the current duration is specified by the discharge of the intrinsic capacitance of the discharge gap. To obtain sustained breakdown at higher p_{He}, the C_0 working capacitance voltage had to be increased from $U = 19$ to 24 kV (the maximum voltage of the primary generator). Despite this, the discharge current decreased with a slightly varying pulse duration $\tau_I = 8-6$ ns. The discharge remains stable without sparking in this mode (at least up to $p_{He} \approx 1$ atm). Photographic images revealed a uniform discharge glow.

With U applied to electrodes $1-1'$ and capacitance C_d excluded (mode B), the voltage pulse duration decreases (~ 8 ns), and the current duration is $\tau_I \approx 10$ ns. The levels of current achieved in this case are almost two times higher at the same voltages. Sparking is not observed up to $p_{He} \approx 300$ Torr; as the working gas pressure increases further, multiple spark channels form in the discharge gap.

Figure 3, *c* shows the dependences of current $I(p_{He})$ through the cuvette and cuvette voltage $U(p_{He})$ at $f = 95$ kHz for modes A and B on helium pressure p_{He}. In both cases, the duration of current pulses does not exceed the time of propagation of the ionization front over the interelectrode distance. The average velocity of the ionization front under similar experimental conditions was $\sim 10^8$ cm/s [4]. A comparison of the achieved discharge parameters demonstrates that, despite the limiting of voltage pulse duration to $\sim 5-6$ ns and the expected improvement in discharge stability, the discharging range does not get extended in the B mode. Mode A with the included C_d capacitance provides a uniform volumetric gas discharge within a wider range of pressures. Apparently, this is attributable to the limiting of the discharge current amplitude and duration. Current amplitude $I \approx 100-50$ A with a peak power of 1800–900 kW could be achieved in the volumetric stage of discharge in mode A at $p_{He} = 0.5-1$ atm.

Thus, the gas discharge regimes in helium at pressures up to atmospheric pressure excited by high-voltage (up to ~ 24 kV) pulses with a rise rate up to 4–5 kV/ns in a burst with repetition rates up to $f = 100$ kHz were examined. A volumetric gas discharge with pulsed currents up to 50 A and an average power up to 1.3 kW was obtained at $p_{He} = 1$ atm. The experimental data demonstrate that a limit imposed on the discharge current allows one to maintain controlled and volumetric current flow at atmospheric helium pressure.

Funding

This study was supported financially by the Russian Science Foundation, grant No. 24-19-00037 (https://rscf.ru/project/24-19-00037/).

Conflict of interest

The authors declare that they have no conflict of interest.

References

[1] T. Shao, Ch. Zhang, *Pulsed discharge plasmas: characteristics and applications* (Springer, 2023). DOI: 10.1007/978-981-99-1141-7

[2] Y. Yin, H. Xu, Y. Zhu, J. Zhuang, R. Ma, D. Cui, Z. Jiao, Appl. Sci., **13**, 12631 (2023). DOI: 10.3390/app132312631

[3] K. Ollegott, P. Wirth, C. Oberste-Beulmann, P. Awakowicz, M. Muhler, Chem. Ing. Tech., **92**, 1542 (2020). DOI: 10.1002/cite.202000075

[4] P.A. Bokhan, P.P. Gugin, M.A. Lavrukhin, D.E. Zakrevsky, I.V. Schweigert, Phys. Plasmas, **30**, 103506 (2023). DOI: 10.1063/5.0164607

[5] P.A. Bokhan, E.V. Belskaya, P.P. Gugin, M.A. Lavrukhin, D.E. Zakrevsky, I.V. Schweigert, Plasma Sources Sci. Technol., **29**, 084001 (2020). DOI: 10.1088/1361-6595/ab9d91

Translated by D.Safin